A molecular triage process mediated by RING finger protein 126 and BCL2-associated athanogene 6 regulates degradation of G_0/G_1 switch gene 2

Received for publication, March 27, 2019, and in revised form, July 19, 2019 Published, Papers in Press, August 1, 2019, DOI 10.1074/jbc.RA119.008544

Kenta Kamikubo[‡], Hisakazu Kato[‡1], Hidetaka Kioka[§], Satoru Yamazaki[¶], Osamu Tsukamoto[‡], Yuya Nishida[‡‖], Yoshihiro Asano[§], Hiromi Imamura[**], Hiroyuki Kawahara[‡‡], Yasunori Shintani[‡], and Seiji Takashima[‡‖2]

From the [‡]Department of Medical Biochemistry, Osaka University Graduate School of Frontier Biosciences, Suita, Osaka 565-0871, Japan, [§]Department of Cardiovascular Medicine, Osaka University Graduate School of Medicine, Suita, Osaka 565-0871, Japan, [¶]Department of Cell Biology, National Cerebral and Cardiovascular Center, Suita, Osaka 565-8565, Japan, [‖]Japan Science and Technology Agency-Core Research for Evolutional Science and Technology (CREST), Kawaguchi, Saitama 332-0012, Japan, [**]Laboratory of Functional Biology, Graduate School of Biostudies, Kyoto University, Kyoto 606-8501, Japan, and [‡‡]Laboratory of Cell Biology and Biochemistry, Department of Biological Sciences, Tokyo Metropolitan University, Tokyo, 192-0397, Japan

Edited by George N. DeMartino

Oxidative phosphorylation generates most of the ATP in respiring cells. ATP is an essential energy source, especially in cardiomyocytes because of their continuous contraction and relaxation. Previously, we reported that G_0/G_1 switch gene 2 (G0S2) positively regulates mitochondrial ATP production by interacting with F_OF_1-ATP synthase. G0S2 overexpression mitigates ATP decline in cardiomyocytes and strongly increases their hypoxic tolerance during ischemia. Here, we show that G0S2 protein undergoes proteasomal degradation via a cytosolic molecular triage system and that inhibiting this process increases mitochondrial ATP production in hypoxia. First, we performed screening with a library of siRNAs targeting ubiquitin-related genes and identified RING finger protein 126 (RNF126) as an E3 ligase involved in G0S2 degradation. RNF126-deficient cells exhibited prolonged G0S2 protein turnover and reduced G0S2 ubiquitination. BCL2-associated athanogene 6 (BAG6), involved in the molecular triage of nascent membrane proteins, enhanced RNF126-mediated G0S2 ubiquitination both *in vitro* and *in vivo*. Next, we found that Glu-44 in the hydrophobic region of G0S2 acts as a degron necessary for G0S2 polyubiquitination and proteasomal degradation. Because this degron was required for an interaction of G0S2 with BAG6, an alanine-replaced G0S2 mutant (E44A) escaped degradation. In primary cultured cardiomyocytes, both overexpression of the G0S2 E44A mutant and RNF126 knockdown effectively attenuated ATP decline under hypoxic conditions. We conclude that the RNF126/BAG6 complex contributes to G0S2 degradation and that interventions to prevent G0S2 degradation may offer a therapeutic strategy for managing ischemic diseases.

Oxygen (O_2) is essential for cell survival because it plays a fundamental role in the production of ATP, mainly through oxidative phosphorylation (OXPHOS).[3] Hypoxia, which is defined as a decrease in O_2 supply, causes the depletion of intracellular ATP and triggers various adaptive cellular responses that maintain the ATP level. For example, hypoxia-exposed cells undergo metabolic switching from OXPHOS toward glycolysis (1–4), but we previously reported that in the early phase of hypoxia, OXPHOS activity rather increases by direct activators such as G_0/G_1 switch gene 2 (G0S2) and HIGD1A (5, 6). We also developed a method to measure mitochondrial ATP concentrations in living cells and showed that G0S2 enhanced mitochondrial ATP production via an interaction with F_OF_1-ATP synthase (5). G0S2 overexpression in cultured cardiomyocytes enhanced mitochondrial ATP production and protected cells from hypoxic damage. These data indicate the therapeutic potential of increasing G0S2 expression for ATP-depleted diseases.

A potential strategy for increasing protein expression is to target the ubiquitin-proteasome system (UPS) to inhibit protein degradation. UPS is the principal mechanism for maintaining cellular protein homeostasis. Ubiquitination, a type of protein posttranslational modification, entails the covalent conjugation of the small ubiquitin protein through the formation of an isopeptide bond between a glycine residue of ubiquitin and lysine residue of the substrate. This reaction occurs through a sequential enzymatic mechanism involving E1 (ubiquitin-activating enzyme), E2 (ubiquitin-conjugating enzyme), and E3 (ubiquitin ligase). E3 is a key enzyme that mediates

This work was supported by the Japan Society for the Promotion of Science (JSPS) KAKENHI Grants JP15H04820 and JP26670402 (to S. T.) and JP15K19378 and JP17K09577 (to H. Kato). This work was also supported by the JSPS through the Funding Program for Next Generation World-Leading Researchers, NEXT Program, CSTP, and JSPS Grant LS079 (to S. T.) and Core Research for Evolutional Science and Technology of the Japan Science and Technology Agency Grant JPMJCR14M2 (CREST, JST) (to S. T.). The authors declare that they have no conflicts of interest with the contents of this article.

This article contains Figs. S1–S5 and Table S1.

[1] To whom correspondence may be addressed. Tel.: 816-6879-3492; Fax: 816-6879-3493; E-mail: katohisa@medbio.med.osaka-u.ac.jp.

[2] To whom correspondence may be addressed. Tel.: 816-6879-3492; Fax: 816-6879-3493; E-mail: takasima@cardiology.med.osaka-u.ac.jp.

[3] The abbreviations used are: OXPHOS, oxidative phosphorylation; G0S2, G0/G1 switch gene 2; UPS, ubiquitin-proteasome system; CFP, cyan fluorescent protein; EGFP,enhanced green fluorescent protein; RNF126, ring finger protein 126; BAG6, BCL2-associated athanogene 6; TA, tail-anchored; ANOVA, analysis of variance.

substrate recognition and is thus responsible for the selectivity and specificity of this system (7). There has been progression recently in the development of therapeutic drugs to specifically inhibit E3 ligase itself or to regulate E3 ligase activity so as to increase the expression of its substrate (8). Because the amount of G0S2 protein is regulated by UPS (9), its degradation process is a potential therapeutic target to increase mitochondrial ATP levels. However, the mechanism regulating the levels of G0S2 protein and the corresponding E3 ligase remains unknown.

In this report, we performed functional screening using an siRNA library and identified RNF126 as a specific E3 ligase for G0S2 degradation. We further demonstrated that the inhibition of G0S2 degradation by RNF126 knockdown or by overexpression of a G0S2 degradation-resistant mutant that sequestered BAG6 preserved mitochondrial ATP concentrations in cardiomyocytes under hypoxic conditions. This result indicates that inhibiting G0S2 degradation may be a novel therapeutic strategy for ATP-depleting conditions such as ischemic heart diseases, mitochondrial diseases, and metabolic diseases.

Results

siRNA screening of ubiquitin ligases for the degradation of G0S2

We first examined G0S2 protein stability in rat neonatal cardiomyocytes. Cells were treated with cycloheximide to inhibit protein synthesis, and the amount of G0S2 protein was analyzed by immunoblotting (Fig. 1*A*). G0S2 was rapidly degraded with a half-life of ~20 min. Proteasome inhibitors, but not lysosomal inhibitors, increased G0S2 protein amounts, indicating degradation by UPS in cardiomyocytes (Fig. 1*B*). Although G0S2 was reported to be regulated by UPS (9), the E3 ligases involved had yet to be identified. Therefore, to identify the E3 ubiquitin ligase specific for G0S2, we performed functional screening using an siRNA library targeting ubiquitin-related genes encoding E1, E2, and E3. We first established C2C12 myoblast cell lines stably expressing EGFP-fused G0S2 to monitor G0S2 protein degradation (C2C12/EGFP-G0S2 cells). Treatment of these cell lines with the proteasome inhibitor MG132 induced G0S2 protein accumulation, which manifested as increased EGFP intensity (Fig. S1*A*). As a positive control for the screening, we selected siRNA for UBA1, an E1 ubiquitin-activating enzyme, and confirmed a 2-fold increase in the fluorescence of EGFP-G0S2 after UBA1 knockdown (Fig. S1*B*). To quantitatively measure the fluorescence intensity of each C2C12/EGFP-G0S2 cell in a high-throughput manner, we used an automated high-content imaging system. In the primary screening, siRNAs from the library were transfected into C2C12/EGFP-G0S2 cells in 96-well plates. After 72-h incubation, cells were imaged and their fluorescence intensities were analyzed (Fig. 1*C*; Table S1). As positive hits, we selected the genes that demonstrated a $\log_2$ -fold change in fluorescence that was greater than 0.6 (Fig. 1*D*). As a counter assay, we established cell lines expressing the EGFP-fused CL1 degron (ACKNWFSSLSHFVIHL) (C2C12/EGFP-CL1 cells), which has been shown to be rapidly degraded by proteasome (10) (Fig. 1*C*; Fig. S1, *C* and *D*; Table S1). The counter assay, together with an assessment of cell number in primary screening (Table S1), identified one gene, *RNF126*, as a candidate for the G0S2-specific E3 ligase (Fig. 1*E*). Because the screening used pools that included four individual siRNAs at once, individual siRNA for RNF126 was separately transfected to C2C12 stably expressing HA-tagged G0S2 cells, and G0S2 protein levels were examined. We confirmed ~60% knockdown of RNF126 by each siRNA (Fig. 1*F*), and G0S2 protein levels were markedly increased by every siRNA (Fig. 1*G*).

RNF126 regulates G0S2 protein degradation by ubiquitination

To examine whether RNF126 acts as an E3 ligase for G0S2 in cells, we used CRISPR-Cas9 technology to generate two RNF126 KO cell lines, specifically RNF126-deficient (RNF126 KO) and RNF126-deficient EGFP-G0S2–expressing (RNF126 KO/EGFP-G0S2) cells (Fig. S2). Endogenous G0S2 protein expression was elevated in RNF126 KO cells (Fig. 2*A*), and RNF126 KO/EGFP-G0S2 cells exhibited an increased EGFP-G0S2 protein half-life as shown by cycloheximide treatment (Fig. 2, *B* and *C*). Next, to examine whether the G0S2 protein accumulation was because of RNF126 deficiency, human RNF126 (hRNF126) was dose-dependently expressed in RNF126 KO cells (Fig. 2*D*). In hRNF126-expressing cells, accumulation of G0S2 protein was decreased. We further tested the *in vivo* ubiquitination of G0S2 in both RNF126 KO cells and control cells. After the transfection of HA-G0S2, cell lysates were subjected to a TUBE2-Agarose pulldown assay, followed by immunoblotting (Fig. 2*E*). A ladder of polyubiquitinated G0S2 was clearly observed in control cells. On the other hand, in RNF126 KO cells, the polyubiquitinated form of G0S2 was decreased (Fig. 2*E*). Re-expression of hRNF126 in RNF126 KO cells restored G0S2 ubiquitination. These data suggest that RNF126 acts as an E3 ligase for G0S2 and specifically regulates its degradation *in vivo*.

Knockdown of RNF126 in neonatal cardiomyocytes preserves mitochondrial ATP production under hypoxia

To investigate the physiological role of RNF126 as a G0S2 E3 ligase, we used primary cultured cardiomyocytes. The knockdown of RNF126 using siRNA in cardiomyocytes confirmed G0S2 protein accumulation without affecting its mRNA expression (Fig. 3, *A* and *B*). In a previous report, we used a mitochondria-targeted FRET-based ATP biosensor, Mit-ATeam, to show that overexpression of G0S2 enhanced mitochondrial ATP production in neonatal cardiomyocytes under hypoxic conditions (5, 11). In the present study, we used this probe to examine whether RNF126 affected mitochondrial ATP production in cardiomyocytes under hypoxic conditions. Because G0S2 expression is induced by hypoxic stimuli, we examined whether hypoxic stimuli change G0S2 turnover. Even under hypoxic condition, G0S2 was also degraded at the same rate of that in normoxic condition (Fig. S3*A*) and its degradation was inhibited by proteasome inhibitor (Fig. S3*B*). Moreover, hypoxic stimuli did not change the protein expression of RNF126 (Fig. S3*C*). We transfected RNF126 siRNA or control siRNA into cardiomyocytes and then infected cells with Mit-ATeam-encoding adenovirus. Forty-eight h after adenovirus

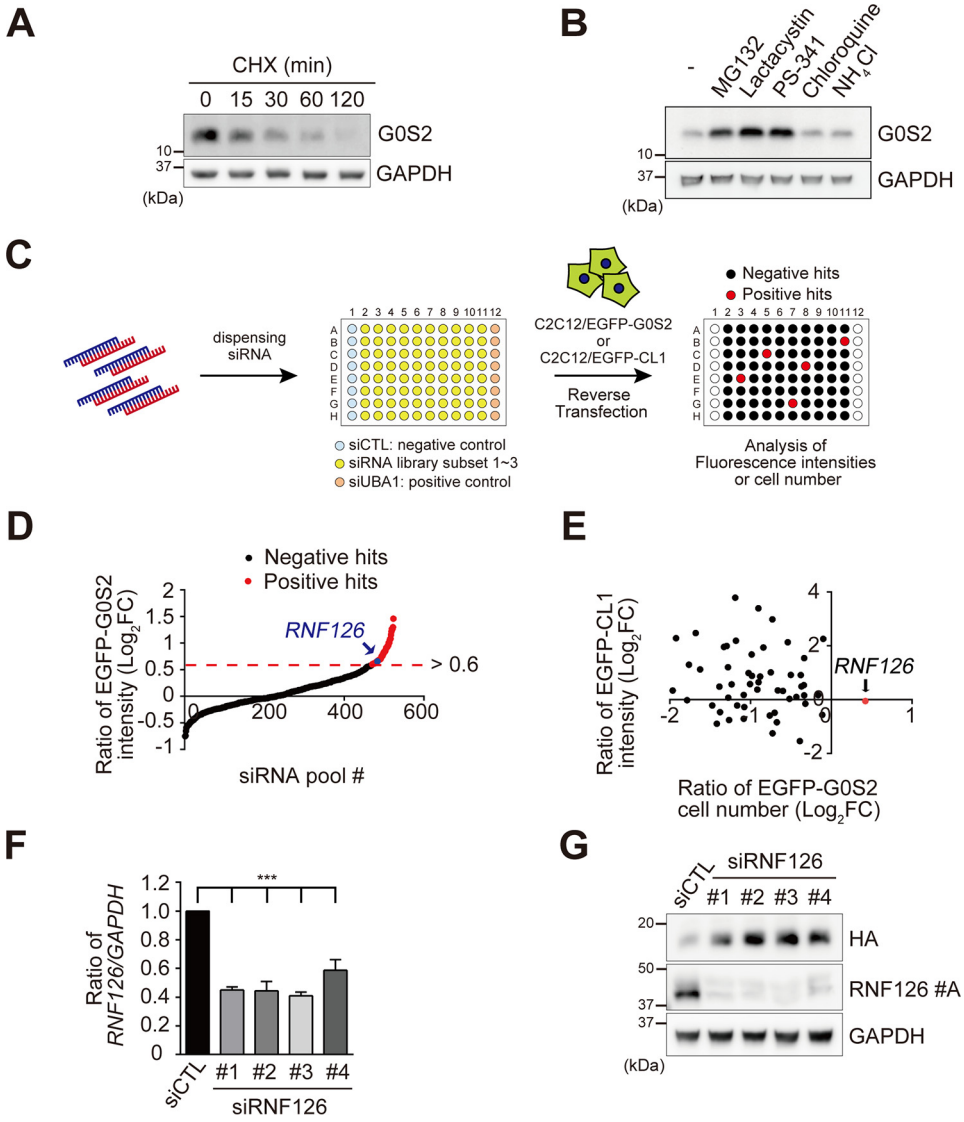

Figure 1. siRNA library screening of ubiquitin ligases for G0S2 degradation. *A*, immunoblot analysis of endogenous G0S2 protein half-life in neonatal rat cardiomyocytes. Cells were treated with cycloheximide (*CHX*) (100 μg/ml) at the indicated times. *B*, immunoblotting of cardiomyocytes treated with proteasome inhibitors (MG132: 10 μM; lactacystin: 10 μM; PS-341: 0.3 μM) or lysosomal inhibitors (chloroquine: 100 μM; NH_4Cl: 10 mM). Four h after the treatment, cells were harvested and subjected to immunoblot analysis. *C*, schematic workflow of siRNA library screening. C2C12 cells stably expressing EGFP-fused G0S2 (C2C12/EGFP-G0S2 cells) or EGFP-fused CL1 degron peptide (C2C12/EGFP-CL1 cells) were transfected with the indicated siRNA. Seventy-two h after transfection, cells were imaged and fluorescence intensities of EGFP were analyzed by IN Cell Analyzer 6000. See also Fig. S1. *D*, distribution of siRNAs ranked according to values of $\log_2$ -fold change (*FC*) of EGFP-G0S2 intensity that is averaged and normalized to the siCTL in three independent experiments. *Black* and *red dots* represent negative and positive hits, respectively. *E*, scatter plot of the $\log_2$ -fold change (*FC*) of EGFP intensity in C2C12/EGFP-CL1 cells and the number of C2C12/EGFP-G0S2 cells, both averaged and normalized to the siCTL in three independent experiments. Each dot represents one siRNA pool targeting one gene. *F*, C2C12 cell lines stably expressing HA-tagged G0S2 (C2C12/HA-G0S2 cells) were transfected with 30 nM either siCTL or siRNF126, as indicated. After 48 h incubation, total RNA was extracted and analyzed by qPCR. Data represent mean values ± S.D. ($n = 3$). ***, $p < 0.001$. *G*, seventy-two h after transfection of siRNA as in (*F*), cells were harvested and subjected to immunoblot analysis. RNF126 was detected by a RNF126 #A antibody.

infection, mitochondrial ATP concentrations were measured by a Mit-ATeam assay during hypoxia. The mitochondrial ATP concentration ($[ATP]_{mito}$) gradually declined in cardiomyocytes transfected with either control or RNF126 siRNA. Notably, the knockdown of RNF126 before the onset of hypoxia reduced this decline in $[ATP]_{mito}$ (Fig. 3, *C* and *D*). These data indicated that increased G0S2 protein levels caused by RNF126 knockdown enhanced mitochondrial ATP production.

BAG6 regulates G0S2 ubiquitination and degradation

RNF126 is a RING finger–type E3 ubiquitin ligase and several substrates of RNF126 have been reported (12–15). In addition, RNF126 was recently reported to be an E3 ligase that degrades mislocalized or tail-anchored transmembrane proteins together with the BAG6-UBL4A-TRC35 complex (16). Thus, we examined the involvement of the BAG6 complex in RNF126-mediated G0S2 degradation. First, we knocked down BAG6 by specific siRNA in neonatal rat cardiomyocytes and C2C12 cells expressing HA-G0S2, then analyzed G0S2 protein amounts. BAG6 knockdown increased G0S2 protein expression in both cardiomyocytes and C2C12 cells (Fig. 4, *A* and *B*) and also inhibited G0S2 ubiquitination (Fig. 4*C*). Cycloheximide chase analysis showed that the half-life of G0S2 was significantly longer than that of control cells in

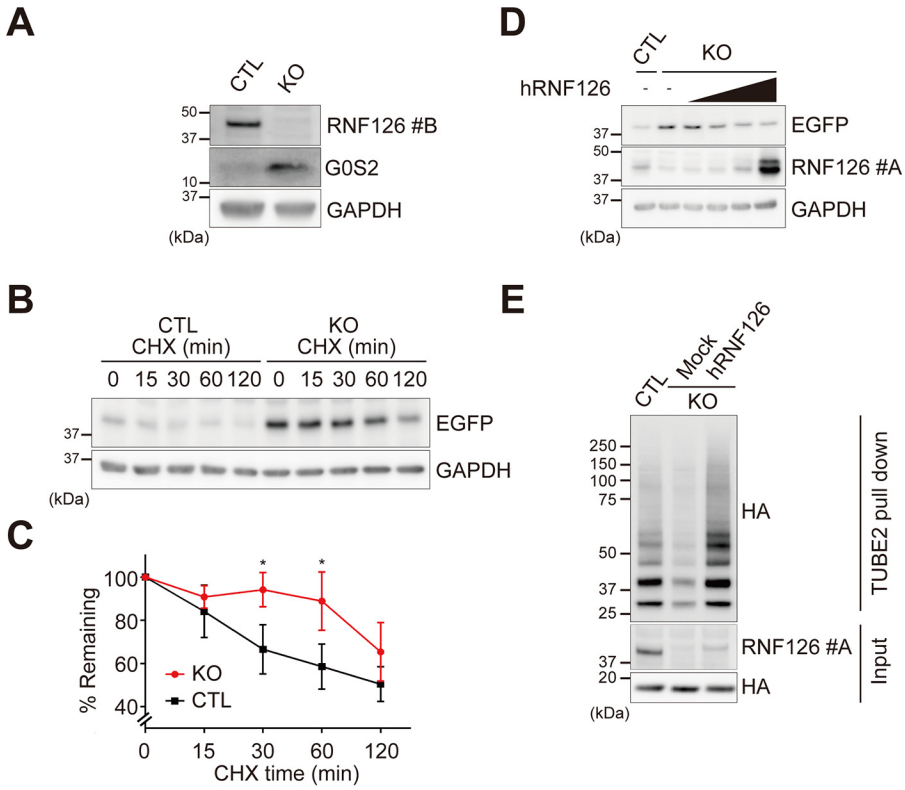

Figure 2. RNF126 regulates G0S2 protein degradation via ubiquitination. *A*, immunoblotting of RNF126 KO cells to confirm the CRISPR-Cas9-mediated genome editing. RNF126 was detected by an RNF126 B antibody. See also Fig. S2. *B*, immunoblotting of RNF126 KO cells or CTL cells stably expressing EGFP-G0S2 treated with cycloheximide (*CHX*) (100 μg/ml) at the indicated times. *C*, each protein level in (*B*) was densitometrically quantified (normalized to 0 min). The asterisks denote statistical significance comparing CTL and RNF126 KO cells. The data represent mean values ± S.D. ($n = 3$). *, $p < 0.05$. *D*, immunoblotting of RNF126 KO cells stably expressing EGFP-G0S2 with or without exogenous expression of human RNF126. *E*, immunoblotting of ubiquitinated HA-G0S2 enriched using tandem ubiquitin binding entity 2 (TUBE2) affinity pulldown in CTL, RNF126 KO, or RNF126 KO cells with exogenous expression of human RNF126. *D* and *E*, for the simultaneous detection of endogenous RNF126 and exogenous RNF126, RNF126 A antibody was used.

BAG6 knocked-down cells (Fig. 4, *D* and *E*). These data suggest that BAG6 is also essential for G0S2 ubiquitination and degradation as a partner protein of RNF126. Furthermore, we examined whether BAG6 knockdown influences mitochondrial ATP decline under hypoxic condition in cardiomyocytes using MitATeam assay. Hypoxia did not affect BAG6 protein expression (Fig. S3*C*). Intriguingly, despite the accumulation of G0S2 protein (Fig. 4*A*), BAG6 knockdown did not affect the mitochondrial ATP production under hypoxia (Fig. 4, *F* and *G*), suggesting that BAG6 acts as not only a part of E3 ligase complex but also a molecular switch of newly synthesized protein (see "Discussion").

Identification of the degron in G0S2

To further reveal the mechanism of G0S2 degradation, it is important to identify the degron in G0S2 that is involved in substrate recognition by the E3 ligase (17, 18). We created several deletion mutants in the N-terminal and C-terminal domains of G0S2, as well as alanine-scanning mutants in the hydrophobic region (Fig. 5*A*). These G0S2 mutants were transfected into C2C12 cells. After treatment with MG132, cell lysates were analyzed by immunoblotting (Fig. 5*B*). Among these mutants, only the Glu-44 to Ala (E44A) mutant was unaffected by MG132, showing a vast increase in basal protein expression. This suggests that amino acid Glu-44 of G0S2 plays an important role in G0S2 degradation. Then, we assessed the *in vivo* ubiquitination and protein half-life of G0S2 E44A. G0S2 E44A was less ubiquitinated (Fig. 5*C*) and had a longer half-life (Fig. 5, *D* and *E*) than the WT. These data suggested that the domain around Glu-44 is a degron of G0S2 that is recognized by the RNF126/BAG6 complex. Thus, we tested the interaction of G0S2 with BAG6 in cells expressing WT or E44A mutant of G0S2. A co-immunoprecipitation experiment revealed that BAG6 preferentially interacted with G0S2 WT rather than with E44A (Fig. 5*F*). These data suggested that BAG6 interacted with G0S2 and recruited RNF126 for ubiquitination.

Because BAG6 not only acts as a scaffold protein of RNF126 but also has a shield-like function to protect the hydrophobic domain of the substrate (19), we considered that BAG6 knockdown or the expression of G0S2 E44A might have caused G0S2 protein aggregation. Thus, to examine the effect of BAG6 knockdown on protein aggregation, C2C12 cells expressing HA-G0S2 WT or E44A were transfected with siRNA for BAG6 and then solubilized with buffer containing 1% Triton X-100. In BAG6-depleted cells, protein aggregates were detected in the detergent-insoluble fraction (20, 21), whereas G0S2 E44A mutant as well as WT existed only in the detergent-soluble fraction (Fig. 5*G*). These data suggest that the G0S2 E44A escaped BAG6-mediated degradation without causing its protein aggregation.

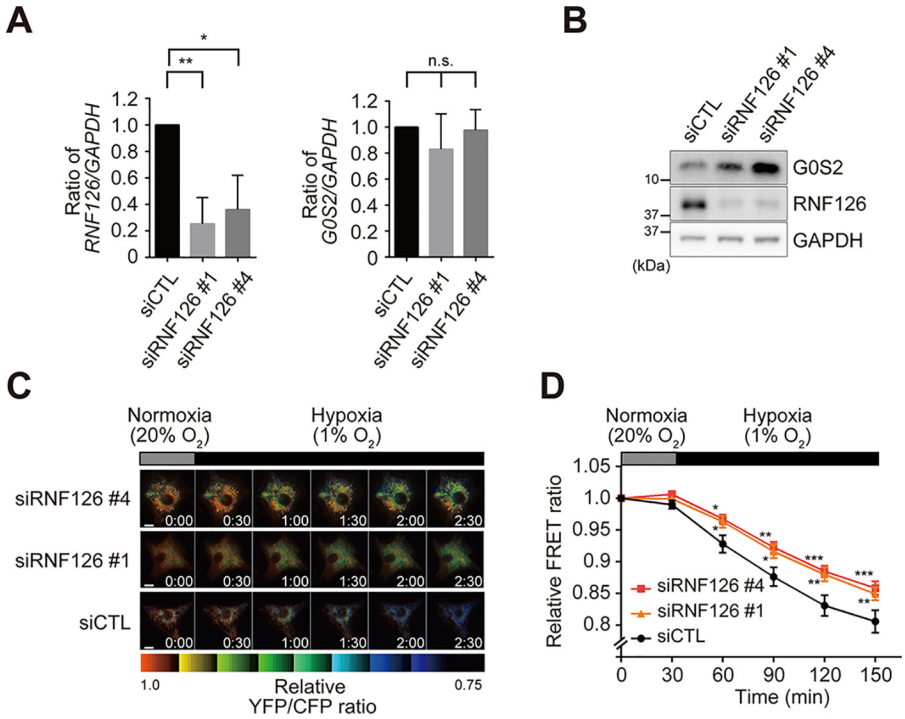

Figure 3. Knockdown of RNF126 in neonatal cardiomyocytes preserves mitochondrial ATP production under hypoxia. *A*, cardiomyocytes were transfected with 30 nM either siCTL or siRNF126, as indicated. After 48 h incubation, total RNA was extracted and analyzed by qPCR. Data represent mean values ± S.D. ($n = 3$). n.s., not significant; *, $p < 0.05$; **, $p < 0.01$. *B*, cardiomyocytes were expressed with the indicated siRNA for 72 h. Cells were harvested and subjected to immunoblotting. See also Fig. S3. *C*, representative YFP/CFP ratiometric pseudocolored images of Mit-ATeam fluorescence in cardiomyocytes expressing the indicated siRNA and adenoviral Mit-ATeam for 48 h. *Scale bar*, 10 μm. *D*, YFP/CFP emission ratio plots of Mit-ATeam fluorescence in cardiomyocytes transfected siCTL ($n = 20$), siRNF126 #1 ($n = 20$), or siRNF126 #4 ($n = 20$) during hypoxia. All measurements were normalized to the ratio at time 0 and compared between cardiomyocytes with siCTL, siRNF126 #1, and #4 at each time point. The asterisks denote statistical significance comparing siRNF126 and siCTL. Data represent mean values ± S.E. *, $p < 0.05$; **, $p < 0.01$; ***, $p < 0.001$.

RNF126 directly ubiquitinates G0S2 in vitro in a BAG6-dependent manner

Next we tested whether the RNF126/BAG6 complex was sufficient to ubiquitinate G0S2 by constructing an *in vitro* ubiquitination assay. We prepared recombinant GST-RNF126 using *Escherichia coli* and recombinant G0S2 and BAG6 from HEK293T cells (Fig. S4, *A–C*). UBCH5B was chosen as the E2 ubiquitin-conjugating enzyme for RNF126 because only the knockdown of UBCH5B increased G0S2 protein expression during our siRNA library screening. Moreover, UBCH5B was reported to act as an E2 enzyme with RNF126 (13, 15, 16). In an *in vitro* ubiquitination assay, recombinant G0S2 was slightly ubiquitinated by GST-RNF126 only in the presence of E1, E2, ATP, and ubiquitin (Fig. 6*A*, *lane 4*). In contrast, the addition of recombinant BAG6 strongly enhanced G0S2 ubiquitination by RNF126 (Fig. 6*A*, *lane 5*; Fig. S4*D*). A catalytically inactive mutant of RNF126 (C231A/C234A, CA) (22), which was created by substituting two critical cysteine residues in a RING domain with alanine residues, did not ubiquitinate G0S2, even in the presence of BAG6 (Fig. 6*B*, *lane 3*). The G0S2 E44A mutant that inhibited BAG6 interaction was less ubiquitinated than the WT, as well as the G0S2 lysine-less mutant (Fig. 6*B*, *lanes 4* and *5*; Fig. S4*E*). We also examined whether G0S2 was ubiquitinated at the type of Lys-48 or Lys-63 linkage by combining an *in vitro* ubiquitination assay and subsequent immunoprecipitation. Immunoblotting with Lys-48 linkage–specific antibody revealed that RNF126 ubiquitinated G0S2 at Lys-48–linked ubiquitination, in consistent with previous reports (Fig. S4*F*) (12, 22). These data indicate that the BAG6 complex is sufficient for G0S2 recognition and ubiquitination.

Inhibition of G0S2 interaction with BAG6 leads to the preservation of mitochondrial ATP concentration in hypoxia

To confirm the importance of BAG6-G0S2 interaction in G0S2 degradation, G0S2 E44A- or WT-encoding lentivirus was expressed in cardiomyocytes. Treatment with proteasome inhibitors results in accumulation of the G0S2 WT protein but not the E44A mutant (Fig. 7*A*). Cycloheximide chase analysis also revealed that compared with WT, the G0S2 E44A mutant had a greatly increased half-life and higher basal protein expression (Fig. 7, *B* and *C*). We next examined the changes in $[ATP]_{mito}$ during hypoxia with the Mit-ATeam assay. Whereas overexpression of G0S2 WT enhanced $[ATP]_{mito}$, as reported previously, G0S2 E44A also enhanced $[ATP]_{mito}$ to a greater extent than WT (Fig. 7, *D* and *E*). We further tested whether this augment of mitochondrial ATP production led to restore the cellular viability in hypoxic stress. The prehypoxia overexpression of G0S2 E44A in cardiomyocytes ameliorated hypoxia-induced cell death (Fig. 7*F*). These results suggest that inhibiting G0S2 degradation via BAG6 sequestration enhances mitochondrial ATP concentration under hypoxic condition and maintains cellular viability.

Discussion

Our recent study showed that G0S2 played an important role in mitochondrial ATP production under hypoxic conditions

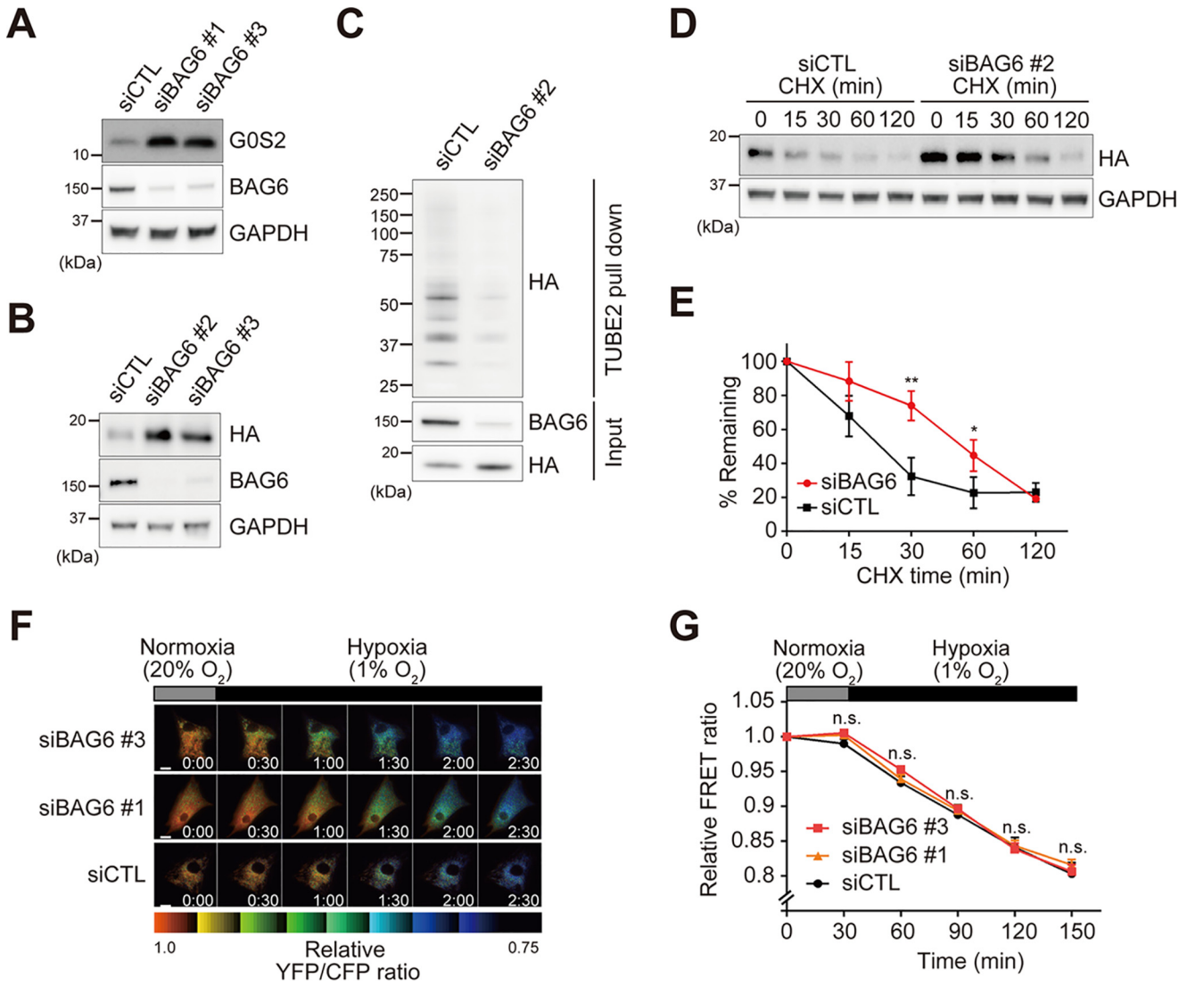

Figure 4. BAG6 regulates G0S2 ubiquitination and degradation. *A–E*, the indicated siRNA was expressed for 72 h in (*A*) cardiomyocytes or (*B–E*) C2C12/HA-G0S2 cells. Cells were harvested and subjected to immunoblotting. *C*, cells were solubilized, and ubiquitinated proteins were enriched by TUBE pulldown assay. *D*, immunoblotting of cells that were treated with cycloheximide at the indicated times (0–120 min). *E*, each protein level in (*D*) was densitometrically quantified (normalized to 0 min) and is shown graphically. The asterisks denote statistical significance comparing siCTL- and siBAG6-treated cells. Data represent mean values ± S.D. ($n = 3$). *, $p < 0.05$; **, $p < 0.01$. *F*, representative YFP/CFP ratiometric pseudocolored images of Mit-ATeam fluorescence in cardiomyocytes expressing the indicated siRNA and adenoviral Mit-ATeam for 48 h. *Scale bar*, 10 μm. *G*, YFP/CFP emission ratio plots of Mit-ATeam fluorescence in cardiomyocytes transfected siCTL ($n = 18$), siBAG6 #1 ($n = 20$), or siBAG6 #3 ($n = 20$) during hypoxia. All measurements were normalized to the ratio at time 0 and compared between cardiomyocytes with siCTL, siBAG6 #1 and #3 at each time point. Data represent mean values ± S.E. *n.s.*, not significant.

(5). Overexpression of G0S2 in cardiomyocytes attenuated the decline in mitochondrial ATP levels during hypoxia and protected cells from hypoxic damage. These results indicate that increasing in G0S2 expression may be a novel therapeutic target for ischemic disease. Thus, for the purpose of developing innovative drugs to increase G0S2 expression, in this study we focused on G0S2 protein turnover.

We demonstrated rapid G0S2 protein degradation in cardiomyocytes and identified RNF126 as an E3 ligase for G0S2 by functional screening using an siRNA library. RNF126 has been implicated in a number of physiological processes, such as mitochondrial metabolic flux (23) and membrane receptor trafficking (22). RNF126 was also shown to directly ubiquitinate and promote the degradation of the cyclin-dependent kinase inhibitor p21 (14) and the mitochondrial iron-sulfur protein frataxin (13), but the mechanism of substrate recognition by RNF126 was not fully understood.

On the other hand, recent studies using an *in vitro* translation system revealed that an RNF126/BAG6 complex targeted mislocalized membrane proteins for proteasomal degradation (16, 19, 24). The mislocalized proteins that failed to be degraded because of BAG6 or RNF126 depletion were rapidly aggregated and accumulated in the cytosol, and these defective proteins are theorized to cause the onset of various diseases (16, 19, 24). Therefore, the RNF126/BAG6 complex plays a major role in the cytosolic pre-emptive quality control system. In this paper, we demonstrated that BAG6 was required for G0S2 ubiquitination and degradation by RNF126. BAG6 knockdown increased G0S2 protein levels and prolonged protein turnover by inhibiting degradation

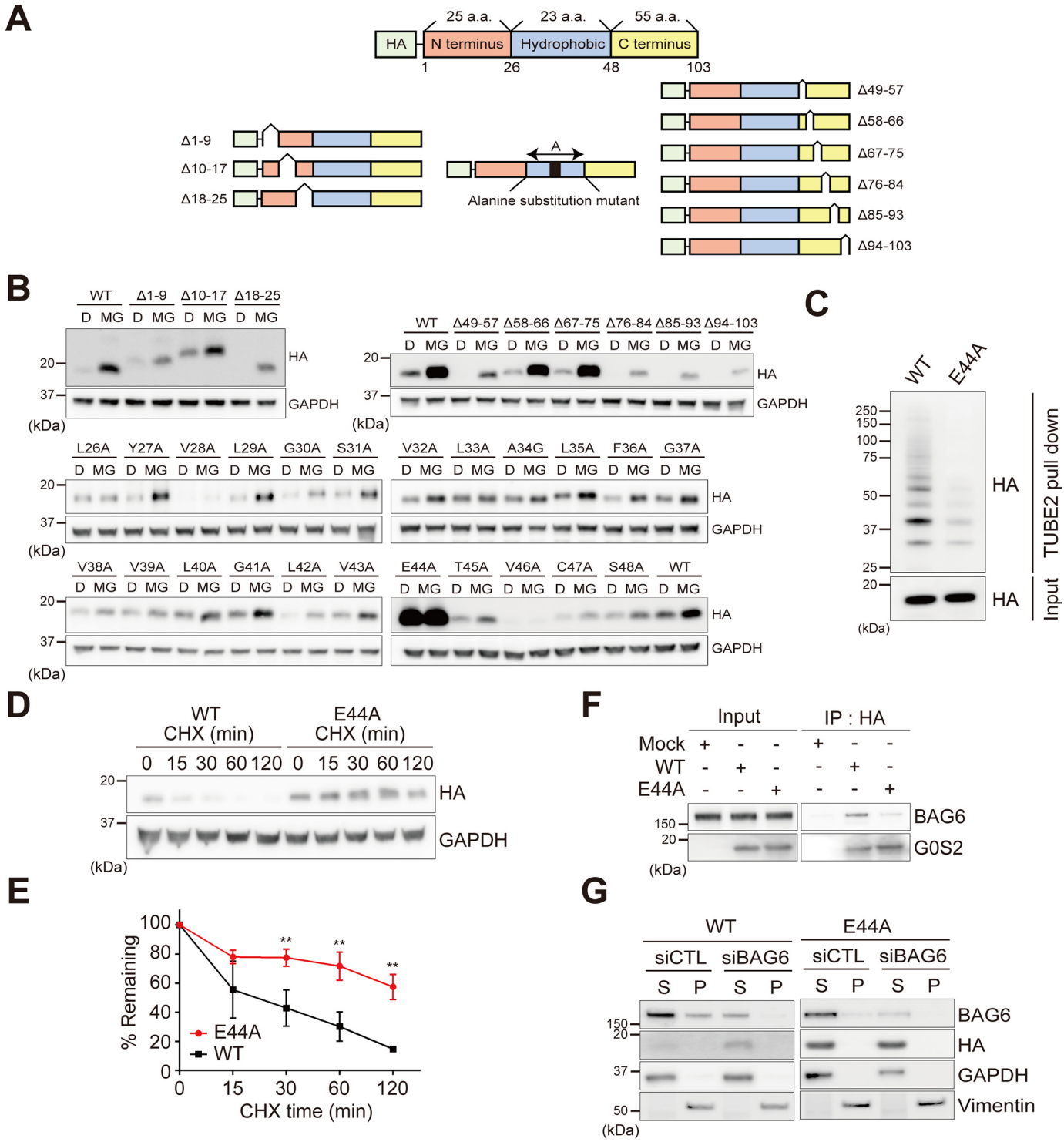

Figure 5. Mutation of the G0S2 degron inhibits its degradation by sequestering BAG6. *A*, schematic diagram of generated mutants. *B*, C2C12 cells were transfected with the indicated G0S2 mutants. After 4-h treatment with DMSO (*D*, 0.1%) or MG132 (*MG*, 10 μM), cells were harvested and subjected to immunoblot analysis. *C*, C2C12/HA-G0S2 WT or E44A cells were solubilized and ubiquitinated proteins were enriched by TUBE2 pulldown assay. *D*, C2C12/HA-G0S2 WT or E44A cells were treated with cycloheximide at the indicated times (0–120 min). *E*, each protein level in (*D*) was densitometrically quantified (normalized to 0 min) and is shown graphically. The asterisks denote statistical significance comparing C2C12/HA-G0S2 WT and E44A cells. Data represent mean values ± S.D. ($n = 3$). **, $p < 0.01$. *F*, immunoprecipitation of HA-G0S2 in HEK293T cells. Cells expressing HA-tagged G0S2 WT or E44A were harvested and immunoprecipitated with anti-HA antibody. *G*, C2C12 cells expressing HA-G0S2 WT or E44A were transfected with the indicated siRNA for 48 h. After solubilizing with the buffer containing 1% Triton X-100, lysates were centrifuged and the supernatant (*S*) and pellet (*P*) fractions were analyzed by immunoblotting. The pellet contains the detergent-insoluble protein aggregates. GAPDH and vimentin are used as the detergent-soluble and -insoluble fractions, respectively.

without causing protein aggregation. Given these data, newly synthesized native G0S2 protein is considered to be constitutively degraded by RNF126 and BAG6 rather than eliminated as a mislocalized protein. Thus, in certain conditions G0S2 may change its conformation or undergo modifications to become a functional protein.

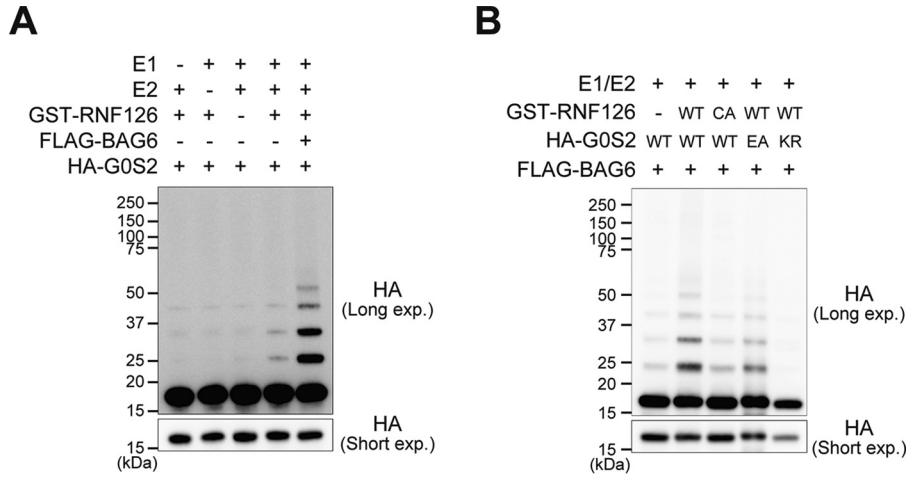

Figure 6. RNF126 directly ubiquitinates G0S2 in vitro in a BAG6-dependent manner. *A*, *in vitro* ubiquitination assay in the presence or absence of purified recombinant UBE1 (E1), UBCH5B (E2), GST-RNF126 (E3), and BAG6, together with His-tagged ubiquitin, ATP, and HA-G0S2 as a substrate. The mixture was incubated for 60 min at 37 °C, and the reaction was stopped by the addition of 3× sample buffer. See also Fig. S4. *B*, *in vitro* ubiquitination assay as in (*A*) except for the use of GST-RNF126 WT or C231A/C234A (*CA*) mutant, and HA-G0S2 WT, E44A, or lysine-less mutant (6KR).

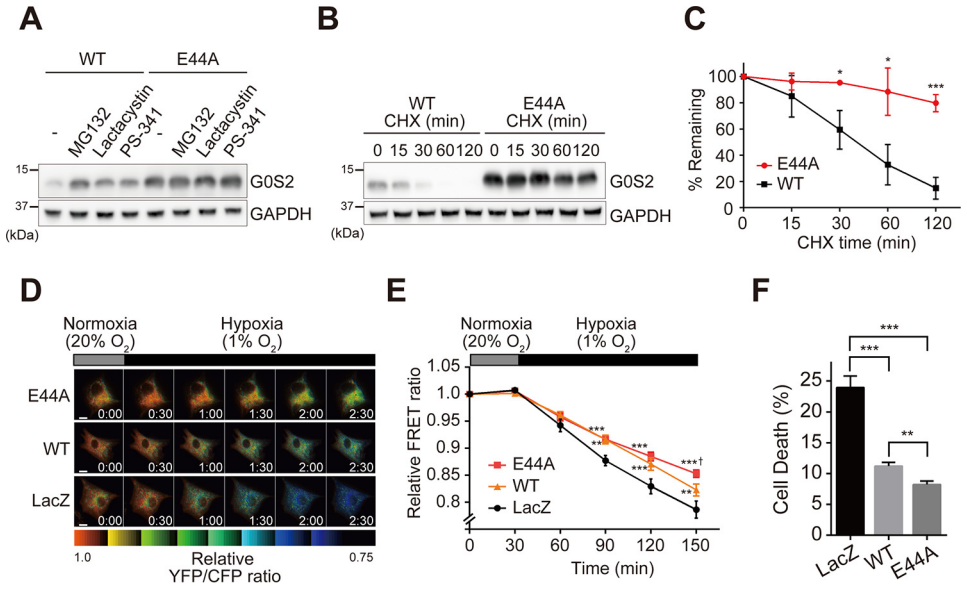

Figure 7. Inhibition of G0S2 interaction with BAG6 leads to the preservation of mitochondrial ATP concentration in hypoxia. *A*, cardiomyocytes expressing G0S2 WT or E44A mutant were treated with proteasome inhibitors (MG132, 10 μM; lactacystin, 10 μM; PS-341, 0.3 μM) for 4 h. Cells were harvested and subjected to immunoblot analysis. *B*, immunoblotting of cells that were treated with cycloheximide at the indicated times (0–120 min). *C*, each protein level of (*B*) was densitometrically quantified (normalized to 0 min) and is shown graphically. The asterisks denote statistical significance comparing G0S2 WT- and E44A-expressing cells. The data represent mean values ± S.D. ($n = 3$). *, $p < 0.05$; ***, $p < 0.001$. *D*, representative YFP/CFP ratiometric pseudocolored images of Mit-ATeam fluorescence in cardiomyocytes expressing the G0S2 WT or E44A mutant and adenoviral Mit-ATeam for 48 h. *Scale bar*, 10 μm. *E*, YFP/CFP emission ratio plots of Mit-ATeam fluorescence in cardiomyocytes expressing lentivirus encoding LacZ ($n = 19$), G0S2 WT ($n = 16$), or G0S2 E44A ($n = 20$) and adenovirus encoding Mit-ATeam during hypoxia. All measurements were normalized to the ratio at time 0 and compared between cardiomyocytes with LacZ, G0S2 WT, and G0S2 E44A at each time point. The asterisks denote statistical significance comparing LacZ and G0S2 WT or E44A mutant. The daggers denote statistical significance comparing G0S2 WT and E44A mutant. Data are represented as the mean ± S.E. **, $p < 0.01$; ***, $p < 0.001$; †, $p < 0.05$. *F*, the bar graph shows the cell death of cardiomyocytes overexpressing G0S2 WT or E44A under hypoxic conditions. Data are represented as the mean ± S.D. ($n = 6$). **, $p < 0.01$; ***, $p < 0.001$.

It was also recently revealed that BAG6 plays a major role as a switching hub in proteasomal degradation or importing proteins into membrane (25). Newly synthesized membrane proteins in ribosomes are first trapped by SGTA and then transferred to the BAG6 complex (BAG6-UBL4A-TRC35). In the case of the tail-anchored (TA) protein, the targeting factor TRC40 delivers the TA protein trapped by SGTA to the endoplasmic reticulum for insertion, whereas BAG6 recruits the E3 ligase RNF126 for protein ubiquitination and degradation (25, 26). Although this precise triage system has been demonstrated using an elegant *in vitro* translation method in previous reports, it remains unclear how it is determined whether newly synthesized TA proteins are degraded or imported into membranes.

Generally, degradation signals within a protein that make it short-lived are called degrons (17, 27). In experiments using deletion mutants and alanine scanning, we determined that Glu-44 is a specific degron within the G0S2 protein. G0S2 has unique hydrophobic region with only one negatively charged glutamic acid. Loss of a negative charge in Glu-44 by alanine

substitution not only increased G0S2 protein stability but also enhanced its role in mitochondrial ATP production. We further revealed that the G0S2 E44A mutant reduced interaction with the BAG6 complex, indicating that this mutant might be more efficiently delivered from the BAG6 complex to subsequent membrane targeting factors. Although some model substrates such as SEC61β or VAMP2 were used to analyze the cytosolic quality control of nascent membrane proteins (19, 25), none of these substrates contains negatively charged amino acids within its transmembrane domain. Therefore, in contrast to general TA proteins, the specific regulatory mechanism of Glu-44–mediated G0S2 degradation, such as masking of its negative charge by binding of an unidentified protein factor, or the posttranslational modification of surrounding residues may be crucial for the escape of G0S2 from the degradation pathway and subsequent membrane targeting that enables appropriate functioning (Fig. S5).

Taken together, we showed that G0S2 protein turnover was regulated by molecular triage system involving RNF126 and BAG6 in the cytosol, although G0S2 does not seem to be a TA protein. Moreover, we identified the degron of G0S2, which is not seen in other substrates of BAG6, and the alanine-replaced mutant inhibited the degradation of G0S2 without aggregation and enhanced mitochondrial ATP production in hypoxia. These findings suggest that further functional analysis may facilitate the development of innovative drugs that inhibit G0S2 degradation by targeting its degron.

Experimental procedures

Reagents and antibody

Reagents were purchased as follows: MG132 (Sigma-Aldrich), lactacystin (Peptide Institute Inc.), PS-341 (Selleck Chemicals), chloroquine (Sigma-Aldrich), ammonium chloride (Wako), cycloheximide (Sigma-Aldrich), Lipofectamine 2000 (Invitrogen), Lipofectamine 3000 (Invitrogen), Lipofectamine RNAiMAX (Invitrogen), anti-HA Agarose (HA-7, Sigma-Aldrich), Anti-FLAG M2 Agarose (Sigma-Aldrich), and TUBE2-Agarose (LifeSensors Inc.). The following antibodies were used in this study: anti-RNF126 (Abcam: RNF126 B, rabbit polyclonal antibody against human RNF126 amino acids 106–119; this antibody reacts with both human and mouse RNF126 but preferentially reacts with human RNF126 compared with mouse one), anti-GAPDH (Merck), anti-His_6 (Clontech), anti-FLAG M2-peroxidase antibody (Sigma-Aldrich), anti-HA (Sigma-Aldrich), anti-GST (Merck), and anti-vimentin (Abcam). mAb against G0S2 was described previously (5). Polyclonal antibody against mouse RNF126 (RNF126 A) was a kind gift from Dr. Nakayama in Tohoku University (12). Polyclonal antibody against BAG6 was described previously (28). All the following recombinant proteins were purchased from R&D Systems: recombinant human ubiquitin, recombinant human ubiquitin–activating enzyme/UBE1, and recombinant human UBCH5B/UBE2D2.

Cell culture and transfection

Primary neonatal cardiomyocytes from 1- or 2-day-old Wister rats were isolated and cultured as described previously (29). C2C12 and HEK293T cells were prepared and cultured in DMEM (Sigma-Aldrich) supplemented with 10% FBS and 1% penicillin-streptomycin. Hypoxic condition (1% O_2) was provided by MCO-5M multi-gas incubator (Sanyo) unless described otherwise. Lipofectamine 2000 and Lipofectamine 3000 were used for plasmid transfection into HEK293T and C2C12 cells, respectively. To knock down endogenous genes, cells were transfected with siRNAs for targeting genes using Lipofectamine RNAiMAX.

Plasmid and viral vector constructions

Mouse G0S2 coding sequence (NM_008059.3) was subcloned into pCDH-EF1 cloning vector with puromycin or G418 resistant gene via 2A peptide (System Biosciences) for plasmid transfection and lentiviral production. The deletion mutants of N-terminal and C-terminal portions of G0S2 or alanine substitution mutants were generated by PCR-based mutagenesis using N-terminal HA-tagged G0S2 WT (HA-G0S2) as a template. N-terminal EGFP ORF was inserted into N terminus of G0S2 by normal restriction enzyme method (EGFP-G0S2). For lentiviral particle production, plasmids encoding various G0S2 WT or mutants were transfected into HEK293T cells together with pRSV-Rev (Addgene no. 12253), pMD 2.G (Addgene no. 12259), and pMDL g/p RRE plasmids (Addgene no. 12251) using Lipofectamine 2000. Seventy-two h after transfection, cell supernatants were collected, and then filtered viral supernatants to remove any nonadherent packaging cells were stocked at −80 °C. Mouse RNF126 (NM_144528.3) and human RNF126 (NM_194460.3) were amplified by PCR from mouse and human heart cDNA, respectively, and subcloned into pCDH-EF1 vector or pENTR1A-Dual selection vector. Adenovirus production was performed as described previously (5). The plasmid encoding human BAG6 (pRK5-FLAG-BAG6) was obtained from Addgene (no. 61836).

siRNA library screening

C2C12 cell lines stably expressing EGFP-fused G0S2 or CL1 degron for siRNA library screening were generated as follows: Lentiviral particles encoding EGFP-G0S2 or EGFP-CL1 (ACKNWFSSLSHFVIHL) were generated as described above and then infected into C2C12 cells, followed by puromycin selection (5 μg/ml, Sigma-Aldrich). Single clones obtained by limiting dilution were used for siRNA library screening. siRNA library screening was performed as follows: For siRNA library screening, we targeted 523 genes encoding factors related to UPS from siGENOME SMART pool siRNA Library-Mouse Ubiquitin Conjugating Subset1~3 (Dharmacon). This library was dissolved in siRNA buffer (60 mM KCl, 6 mM HEPES, 0.9 mM $MgCl_2$) to adjust final concentration in 1 μM and dispensed with each well containing 3 pmol of a pool in 96-well plate. siUBA1 and siCTL were used as the positive and negative controls, respectively. Transfection reagent Lipofectamine RNAiMAX was first added to siRNA library-containing plates according to the manufacturer's protocol. After incubation in brief, C2C12/EGFP-G0S2 or C2C12/EGFP-CL1 cells were seeded onto 96-well plates with the appropriate cell numbers. Twenty-four h after transfection, media were changed to FluoroBrite DMEM (Gibco) supplemented with 10% FBS, 1% penicillin-streptomycin, and 1× GlutaMax to avoid the toxicity of

transfection reagent, and cells were incubated for additional 48 h. After staining nuclei with Hoechst 33342, cells were imaged using IN Cell Analyzer 6000 (GE Healthcare), and EGFP fluorescence intensities or cell numbers of each well were quantitatively analyzed by Developer ToolBox (GE Healthcare). Each assay was performed and normalized to the siCTL in three independent experiments. The following siRNAs were used in this study: siUBA1, CACUUACUUUUGAUGUUAA; siRNF126#1, UCACGCAGCUCCUCAAUCA; siRNF126#2, GCAACCACCUGUUCCACGA; siRNF126#3, CAUCUUCGACGAUAGCUUU; siRNF126#4, UCACGCUGCCACAGGGAUA; siBAG6#1, GGGUACCUAUUAUCCAGCA; siBAG6#2, CCUUCAAUCUUCCUAGUGA; siBAG6#3, GCACAUGAUUAGGGAUAUA.

RNA extraction and quantitative RT-PCR

Total RNA was extracted from C2C12/HA-G0S2 using RNA-Bee Reagent (Tel-Test) and converted to cDNA using the High Capacity cDNA Reverse Transcription Kit (Applied Biosystems) according to the manufacturer's instructions. Quantitative RT-PCR was performed with SYBR technology and Step One Plus Real-Time PCR Systems (Applied Biosystems). All of the samples were processed in duplicate. The level of each transcript was quantified by the threshold cycle method using GAPDH as an endogenous control.

Generation of RNF126 KO cells using CRISPR/Cas9 system

Plasmids encoding single guide RNA (no. 67974) and Cas9 (no. 68343) for lentiviral production were obtained from Addgene. Lentiviral particles encoding Cas9 were generated and then infected into C2C12 cells, followed by selection with blasticidin (20 μg/ml, Wako) (C2C12/Cas9). RNF126 KO cell lines of only RNF126-deficient cells were generated as follows: The single guide RNA sequence corresponding to mouse RNF126 gene (5′-GTGCGAGTCTGGCTTCATTGAGG-3′) was subcloned into pKLV2-U6gRNA5(BbsI)-PGKpuro2ABFP-W Vector (Addgene no. 67974) by normal restriction enzyme method, and then lentiviral particles were generated as described above. Lentiviral particles encoding RNF126 guide RNA were infected into C2C12/Cas9 cells and then selected with puromycin (5 μg/ml) (C2C12/Cas9/RNF126 KO). RNF126-deficient EGFP-G0S2-expressing cells were generated as follows: Lentiviral particles encoding EGFP-G0S2 fused with the G418 resistant gene was infected into C2C12/Cas9 cells and then selected with G418 (0.8 mg/ml) (C2C12/Cas9/EGFP-G0S2). Lentiviral particles encoding RNF126 guide RNA were infected into C2C12/Cas9/EGFP-G0S2 and selected with puromycin (5 μg/ml) (C2C12/Cas9/EGFP-G0S2/RNF126 KO).

Protein purification

Recombinant HA-G0S2 proteins (WT, E44A, 6KR) or FLAG-BAG6 were purified as follows: HEK293T cells transfected with HA-G0S2 plasmids or FLAG-BAG6 were lysed with buffer A (50 mM Tris-HCl pH 7.5, 150 mM NaCl, 1 mM EDTA and Protease Inhibitor Cocktail (Nacalai-Tesque)) containing 0.5% Nonidet P-40 and immunoprecipitated with anti-HA Agarose or anti-FLAG M2-Agarose, respectively, at 4 °C for 1 h. After extensive washing, the proteins were eluted three times with HA or FLAG peptide. Recombinant GST-fused RNF126 proteins (WT and C231A/C234A) were purified as follows: The mouse RNF126 cDNA was subcloned into pGEX-6P-1 Vector. The RING domain mutant (C231A/C234A) was generated by PCR-based mutagenesis using pGEX-6P-1/RNF126 WT as a template. pGEX-6P1/RNF126 WT or RNF126 C231A/C234A mutant was transformed into BL21-Rosetta chemically competent *E. coli* (Invitrogen), and then protein expression was induced with 0.5 mM isopropyl β-D-1-thiogalactopyranoside (Sigma-Aldrich) at 15 °C for 6 h. The cells were collected by centrifugation and lysed by sonication in buffer A. After addition of 2% Triton X-100, the cell lysates were agitated at 4 °C for 30 min and pulled down with GSH-Sepharose 4 Fast Flow (GE Healthcare) at 4 °C for 1 h. After being washed three times, the proteins were eluted with 10 mM reduced GSH and ultrafiltered in buffer A using a Nanosep 50K Device (Pall Corp.).

In vivo/in vitro ubiquitination of G0S2

In vivo ubiquitination assay was performed as follows: C2C12/HA-G0S2 or RNF126 KO cells were lysed with buffer A containing 0.5% Nonidet P-40 and immunoprecipitated with TUBE2-Agarose at 4 °C, for 4 h. After extensive washing, proteins were eluted with SDS sample buffer. *In vitro* ubiquitination assay was performed as follows: *in vitro* ubiquitination assay was performed in a mixture containing 50 nM human ubiquitin-activating enzyme (UBE1), 250 nM human UBCH5B (UBE2D2), 2.5 nM purified GST-RNF126, 50 nM purified FLAG-BAG6 from 293T cells, and 73.5 nM purified HA-G0S2 from 293T cells in reaction buffer (50 mM Tris-HCl, pH 7.5, 5 mM $MgCl_2$, 2 mM ATP, 1 mM DTT, 10 μM ubiquitin, 100 μM $ZnCl_2$) at 37 °C for 60 min. Reaction was stopped by adding SDS sample buffer. Samples were electrophoresed and analyzed with immunoblotting.

Preparation of detergent-soluble and -insoluble fraction

C2C12 cells were transfected with 30 nM either siCTL or siBAG6. Forty-eight h after transfection, HA-G0S2 WT or E44A was transfected into cells expressing siRNA. Forty-eight h after plasmid transfection, cells were treated with 10 μM MG132 for 4 h and harvested with buffer A containing 1% Triton X-100. Cell lysates were centrifuged at 20,000 × *g* for 20 min at 4 °C, and the resulting precipitates were dissolved in SDS sample buffer in equivalent to a supernatant.

FRET-based measurement of mitochondrial ATP concentration (Mit-ATeam assay)

FRET-based measurement of mitochondrial ATP concentration in cardiomyocytes was measured as described previously (5). Briefly, FRET signal was measured in cardiomyocytes infected with adenoviral encoding Mit-ATeam 1.03 with an Olympus IX-81 inverted fluorescence microscopy (Olympus) using a PL APO 60×, 1.35 N.A., oil immersion objective lens (Olympus). Mit-ATeam assay was performed under 1% O_2 condition at 48 h after siRNA transfection or lentivirus infection.

Cell viability assay

Cardiomyocytes seeded on 96-well plates were infected with lentivirus encoding G0S2 WT or E44A mutant for 24 h, and then they were exposed to hypoxia for 24 h. Hypoxic condition (less than 0.1%) was achieved by the AneroPack System (Mitsubishi Gas Chemical, Inc.). After hypoxia, cells were stained with 1 μg/ml propidium iodide (Sigma-Aldrich) and 0.5 μg/ml Hoechst 33342 (Dojin Chemical, Inc.) at 37 °C for 30 min. The stained nuclei were then imaged using IN Cell Analyzer 6000. The data were analyzed as percentage of propidium iodide–positive nuclei/total nuclei.

Quantification and statistical analysis

Our data are expressed as mean ± S.D. of at least three independent experiments except for Mit-ATeam assay as mean ± S.E. The two-tailed Student's *t* test was used to analyze differences between two groups unless otherwise noted. For the data shown in Fig. 1*F*, one-way ANOVA with Dunnett's post hoc test was used to compare multiple groups with siCTL. For the data of Mit-ATeam, as shown in Figs. 3*D*, 4*G*, and 7*E*, two-way ANOVA with Tukey-Kramer's test was used for comparisons of multiple groups at individual time points. For the data shown in Fig. 7*F*, one-way ANOVA with Tukey-Kramer's test was used.

Author contributions—K. K., S. Y., and O. T. investigation; H. Kato conceptualization; H. Kato writing-original draft; H. Kato and S. T. project administration; H. Kioka and Y. A. methodology; Y. N., H. I., and Y. S. resources; Y. A. data curation; H. Kawahara formal analysis; S. T. supervision.

Acknowledgments—We thank Dr. Keiko Nakayama (Tohoku University) for the kind gift of anti-RNF126 antibody. We also thank E. Nakai, E. Takata, S. Gion, K. Shingu, Y. Uegaki, and M. Kishimoto for technical assistance and Y. Okada, Y. Kurokawa, and H. Kawasaki for secretarial work.

References

1. Semenza, G. L. (2012) Hypoxia-inducible factors in physiology and medicine. *Cell* **148,** 399–408 CrossRef Medline
2. Papandreou, I., Cairns, R. A., Fontana, L., Lim, A. L., and Denko, N. C. (2006) HIF-1 mediates adaptation to hypoxia by actively down-regulating mitochondrial oxygen consumption. *Cell Metab.* **3,** 187–197 CrossRef Medline
3. Kim, J. W., Tchernyshyov, I., Semenza, G. L., and Dang, C. V. (2006) HIF-1-mediated expression of pyruvate dehydrogenase kinase: A metabolic switch required for cellular adaptation to hypoxia. *Cell Metab.* **3,** 177–185 CrossRef Medline
4. Semenza, G. L., Jiang, B. H., Leung, S. W., Passantino, R., Concordet, J. P., Maire, P., and Giallongo, A. (1996) Hypoxia response elements in the aldolase A, enolase 1, and lactate dehydrogenase A gene promoters contain essential binding sites for hypoxia-inducible factor 1. *J. Biol. Chem.* **271,** 32529–32537 CrossRef Medline
5. Kioka, H., Kato, H., Fujikawa, M., Tsukamoto, O., Suzuki, T., Imamura, H., Nakano, A., Higo, S., Yamazaki, S., Matsuzaki, T., Takafuji, K., Asanuma, H., Asakura, M., Minamino, T., Shintani, Y., *et al.* (2014) Evaluation of intramitochondrial ATP levels identifies G0/G1 switch gene 2 as a positive regulator of oxidative phosphorylation. *Proc. Natl. Acad. Sci. U.S.A.* **111,** 273–278 CrossRef Medline
6. Hayashi, T., Asano, Y., Shintani, Y., Aoyama, H., Kioka, H., Tsukamoto, O., Hikita, M., Shinzawa-Itoh, K., Takafuji, K., Higo, S., Kato, H., Yamazaki, S., Matsuoka, K., Nakano, A., Asanuma, H., *et al.* (2015) Higd1a is a positive regulator of cytochrome c oxidase. *Proc. Natl. Acad. Sci. U.S.A.* **112,** 1553–1558 CrossRef Medline
7. Hershko, A., and Ciechanover, A. (1998) The ubiquitin system. *Annu. Rev. Biochem.* **67,** 425–479 CrossRef Medline
8. Wertz, I. E., and Wang, X. (2019) From discovery to bedside: Targeting the ubiquitin system. *Cell Chem. Biol.* **26,** 156–177 CrossRef Medline
9. Heckmann, B. L., Zhang, X., Saarinen, A. M., and Liu, J. (2016) Regulation of G0/G1 switch gene 2 (G0S2) protein ubiquitination and stability by triglyceride accumulation and ATGL interaction. *PLoS One* **11,** e0156742 CrossRef Medline
10. Bence, N. F., Sampat, R. M., and Kopito, R. R. (2001) Impairment of the ubiquitin-proteasome system by protein aggregation. *Science* **292,** 1552–1555 CrossRef Medline
11. Imamura, H., Nhat, K. P. H., Togawa, H., Saito, K., Iino, R., Kato-Yamada, Y., Nagai, T., and Noji, H. (2009) Visualization of ATP levels inside single living cells with fluorescence resonance energy transfer-based genetically encoded indicators. *Proc. Natl. Acad. Sci. U.S.A.* **106,** 15651–15656 CrossRef Medline
12. Ishida, N., Nakagawa, T., Iemura, S. I., Yasui, A., Shima, H., Katoh, Y., Nagasawa, Y., Natsume, T., Igarashi, K., and Nakayama, K. (2017) Ubiquitylation of Ku80 by RNF126 promotes completion of nonhomologous end joining-mediated DNA repair. *Mol. Cell. Biol.* **37,** e00347-16 CrossRef Medline
13. Benini, M., Fortuni, S., Condò, I., Alfedi, G., Malisan, F., Toschi, N., Serio, D., Massaro, D. S., Arcuri, G., Testi, R., and Rufini, A. (2017) E3 ligase RNF126 directly ubiquitinates frataxin, promoting its degradation: identification of a potential therapeutic target for Friedreich ataxia. *Cell Rep.* **18,** 2007–2017 CrossRef Medline
14. Wang, L., Wang, X., Zhao, Y., Niu, W., Ma, G., Yin, W., and Shi, C. (2016) E3 ubiquitin ligase RNF126 regulates the progression of tongue cancer. *Cancer Med.* **5,** 2043–2047 CrossRef Medline
15. Zhi, X., Zhao, D., Wang, Z., Zhou, Z., Wang, C., Chen, W., Liu, R., and Chen, C. (2013) E3 ubiquitin ligase RNF126 promotes cancer cell proliferation by targeting the tumor suppressor p21 for ubiquitin-mediated degradation. *Cancer Res.* **73,** 385–394 CrossRef Medline
16. Rodrigo-Brenni, M. C., Gutierrez, E., and Hegde, R. S. (2014) Cytosolic quality control of mislocalized proteins requires RNF126 recruitment to Bag6. *Mol. Cell* **55,** 227–237 CrossRef Medline
17. Ravid, T., and Hochstrasser, M. (2008) Diversity of degradation signals in the ubiquitin-proteasome system. *Nat. Rev. Mol. Cell Biol.* **9,** 679–690 CrossRef Medline
18. Guharoy, M., Bhowmick, P., Sallam, M., and Tompa, P. (2016) Tripartite degrons confer diversity and specificity on regulated protein degradation in the ubiquitin-proteasome system. *Nat. Commun.* **7,** 10239 CrossRef Medline
19. Hessa, T., Sharma, A., Mariappan, M., Eshleman, H. D., Gutierrez, E., and Hegde, R. S. (2011) Protein targeting and degradation are coupled for elimination of mislocalized proteins. *Nature* **475,** 394–397 CrossRef Medline
20. Wang, Q., Liu, Y., Soetandyo, N., Baek, K., Hegde, R., and Ye, Y. (2011) A ubiquitin ligase-associated chaperone holdase maintains polypeptides in soluble states for proteasome degradation. *Mol. Cell* **42,** 758–770 CrossRef Medline
21. Minami, R., Hayakawa, A., Kagawa, H., Yanagi, Y., Yokosawa, H., and Kawahara, H. (2010) BAG-6 is essential for selective elimination of defective proteasomal substrates. *J. Cell Biol.* **190,** 637–650 CrossRef Medline
22. Smith, C. J., Berry, D. M., and McGlade, C. J. (2013) The E3 ubiquitin ligases RNF126 and Rabring7 regulate endosomal sorting of the epidermal growth factor receptor. *J. Cell Sci.* **126,** 1366–1380 CrossRef Medline
23. Yoshino, S., Hara, T., Nakaoka, H. J., Kanamori, A., Murakami, Y., Seiki, M., and Sakamoto, T. (2016) The ERK signaling target RNF126 regulates anoikis resistance in cancer cells by changing the mitochondrial metabolic flux. *Cell Discov.* **2,** 16019 CrossRef Medline
24. Juszkiewicz, S., and Hegde, R. S. (2018) Quality control of orphaned proteins. *Mol. Cell* **71,** 443–457 CrossRef Medline
25. Shao, S., Rodrigo-Brenni, M. C., Kivlen, M. H., and Hegde, R. S. (2017) Mechanistic basis for a molecular triage reaction. *Science* **355,** 298–302 CrossRef Medline

26. Guna, A., and Hegde, R. S. (2018) Transmembrane domain recognition during membrane protein biogenesis and quality control. *Curr. Biol.* **28,** R498–R511 CrossRef Medline
27. Varshavsky, A. (1991) Naming a targeting signal. *Cell* **64,** 13–15 CrossRef Medline
28. Yamamoto, K., Hayashishita, M., Minami, S., Suzuki, K., Hagiwara, T., Noguchi, A., and Kawahara, H. (2017) Elimination of a signal sequence-uncleaved form of defective HLA protein through BAG6. *Sci. Rep.* **7,** 14545 CrossRef Medline
29. Seguchi, O., Takashima, S., Yamazaki, S., Asakura, M., Asano, Y., Shintani, Y., Wakeno, M., Minamino, T., Kondo, H., Furukawa, H., Nakamaru, K., Naito, A., Takahashi, T., Ohtsuka, T., Kawakami, K., *et al.* (2007) A cardiac myosin light chain kinase regulates sarcomere assembly in the vertebrate heart. *J. Clin. Invest.* **117,** 2812–2824 CrossRef Medline